Entropy **2014**, *16*, 2549-2567; doi:10.3390/e16052549

OPEN ACCESS

entropy

ISSN 1099-4300

www.mdpi.com/journal/entropy

Article

Exergy Analysis of Flat Plate Solar Collectors

Zhong Ge [1], Huitao Wang [1,*], Hua Wang [1], Songyuan Zhang [1] and Xin Guan [2]

[1] Engineering Research Center of Metallurgical Energy Conservation and Emission Reduction, Ministry of Education Kunming University of Science and Technology, Kunming 650093, China; E-Mails: zhongge@hotmail.com(Z.G.); wanghuaheat@hotmail.com(H.W.); zsy_88@126.com(S.Y.Z.)

[2] School of Energy and power Engineering, University of Shanghai For Science and Technology, Shanghai 200093, China; E-Mail: cindy-guan@163.com

* Author to whom correspondence should be addressed; E-Mail: energywht@sina.com; Tel.: +86-0871-65153405.

Received: 19 November 2013; in revised form: 1 April 2014 / Accepted: 5 May 2014 / Published: 9 May 2014

Abstract: This study proposes the concept of the local heat loss coefficient and examines the calculation method for the average heat loss coefficient and the average absorber plate temperature. It also presents an exergy analysis model of flat plate collectors, considering non-uniformity in temperature distribution along the absorber plate. The computation results agree well with experimental data. The effects of ambient temperature, solar irradiance, fluid inlet temperature, and fluid mass flow rate on useful heat rate, useful exergy rate, and exergy loss rate are examined. An optimal fluid inlet temperature exists for obtaining the maximum useful exergy rate. The calculated optimal fluid inlet temperature is 69 °C, and the maximum useful exergy rate is 101.6 W. Exergy rate distribution is analyzed when ambient temperature, solar irradiance, fluid mass flow rate, and fluid inlet temperature are set to 20 °C, 800 W/m^2, 0.05 kg/s, and 50 °C, respectively. The exergy efficiency is 5.96%, and the largest exergy loss is caused by the temperature difference between the absorber plate surface and the sun, accounting for 72.86% of the total exergy rate.

Keywords: flat plate collector; heat loss coefficient; exergy; exergy loss

---

1. Introduction

Solar energy, a clean and renewable energy source with no harmful environmental effects, has received considerable attention for generating heat and electricity [1,2]. The flat plate solar collector is the main component of solar heating systems. Thus, the performance of the plate solar collector is important. To analyze the performance of solar collectors, the energy equation alone does not account for internal losses, so it is not a sufficient criterion for flat plate solar collector efficiency [3]. Therefore, an analysis based on the second law of thermodynamics that determines the exergy of the system is necessary. The effect of some vital parameters on the exergy of flat plate collectors is also necessary to optimize solar system design and operation.

Solar collectors have been examined in terms of their exergy, exergy efficiency, and entropy generation [4–6]. Bejan *et al.* conducted an exergy analysis of a solar collector and found that the amount of exergy delivered by solar collector systems is affected by heat transfer irreversibilities [7]. Suzuki compared flat plate and evacuated tube collectors in terms of exergy [8]. Jafarkazemi *et al.* conducted both energy and exergy analyses of a flat plate solar collector [9]. Luminosu and Fara proposed an exergy analysis of a flat plate solar collector based on the assumption that fluid inlet temperature is equal to ambient temperature [10]. Farahat *et al.* attempted to determine the optimum values of the mass flow rate, absorber plate area, and maximum exergy efficiency of a flat plate collector [11]. Akpinar *et al.* experimentally compared a flat plate solar air heater with several obstacles and one without and found that the efficiency of solar air collectors significantly depends on the solar radiation, the surface geometry of the collectors, and the extension of the air flow line [12]. Alta *et al.* experimentally compared three plate solar air heaters based on energy and exergy output and found that the heater with double glass covers and fins is more effective than the other two heaters [13]. In all of these studies, however, collector performance was evaluated without considering non-uniformity in the temperature distribution of the absorber plate or even assuming a constant overall heat loss coefficient.

The present work presents a theoretical model considering non-uniformity in temperature distribution along the absorber plate for the exergy analysis of flat plate solar collectors. The model has also been experimentally verified.

2. Theoretical Model

2.1. Energy Equation for Flat Plate Solar Collectors

A micro unit dA is taken from the absorber plate in steady state according to the first law of thermodynamics [14]:

$$\delta Q_u = \delta Q_s - \delta Q_l = \left[S - U_l \left(T_p - T_a \right) \right] dA \tag{1}$$

where Q_u is the useful heat rate gain of the flat plate solar collector, Q_s is the radiation flux absorbed by the absorber plate, Q_l is the heat loss from the solar collector to the environment, S is the radiation flux absorbed by a unit area of the absorber plate, U_l is the local heat loss coefficient of dA, T_p is the temperature of dA, and T_a is the ambient temperature.

According to the integral mean value theorem, the following can be deduced from Equation (1):

$$Q_u = \iint_{A_p} \left[S - U_l \left(T_p - T_a \right) \right] dA = A_p \left[S - \overline{\overline{U_l}} \left(\overline{\overline{T_p}} - T_a \right) \right] \tag{2}$$

where A_p is the area of the absorber plate, $\overline{\overline{U_l}}$ is the integral average of U_l over the absorber plate, and $\overline{\overline{T_p}}$ is the integral average of T_p over the absorber plate.

2.2. Calculation Methodology for Average Heat Loss Coefficient and Average Absorber Plate Temperature

To simplify the model, the following assumptions are made:

(1) The plate is in a steady-state heat transfer condition.
(2) The temperature gradient in the direction of the fin thickness is negligible.
(3) The fluid mass flow rate inside metal tubes is uniform.
(4) The pressure drop of the fluid inside metal tubes is neglected.

The absorber plate is composed of metal tubes and fins, it is shown in Figure 1:

Figure 1. Absorber plate consisting of metal tubes and fins.

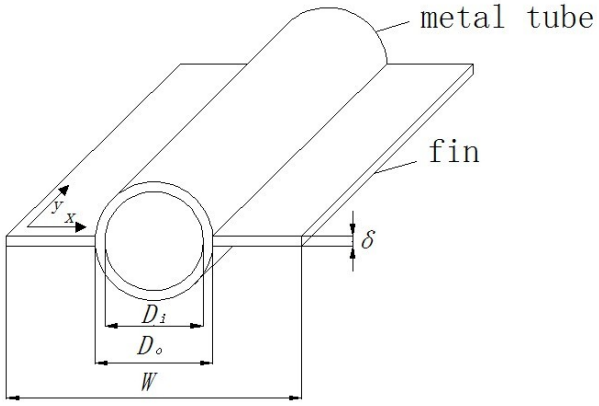

Establishing coordinate system as Figure 1, a micro unit *dy* is taken from the absorber plate. The heat transferred from the absorber plate to the glass comprises radiative heat and convective heat. The radiative heat transfer from the absorber plate to the glass of *dy* is:

$$\delta q_{r,p-1} = \frac{\sigma \left(\overline{T_p}^4 - T_1^4 \right)}{\frac{1-\varepsilon_p}{\varepsilon_p W} + \frac{1}{W} + \frac{1-\varepsilon_1}{\varepsilon_1 W}} dy \tag{3}$$

where W is the width of the metal tube and fins (tube center to center distance), σ is the Stefan–Boltzmann constant, $\overline{T_p}$ is the average temperature of *dy*, T_1 is the temperature of the glass, ε_p is the emissivity of the absorber plate, and ε_1 is the emissivity of the glass.

The convective heat transfer coefficient between the absorber plate and the glass is calculated from the Nusselt number according to the following Equation [15]:

$$Nu = 1 + 1.44\left\{\left[\left|1 - \frac{1708}{Ra\cos\theta}\right| + (1 - \frac{1708}{Ra\cos\theta})\right]/2\right\}\left[1 - \frac{(\sin 1.8\theta)^{1.6}\,1708}{Ra\cos\theta}\right] + \left\{\left|\left(\frac{Ra\cos\theta}{5830}\right)^{1/3} - 1\right| + \left[\left(\frac{Ra\cos\theta}{5830}\right)^{1/3} - 1\right]\right\}/2 \tag{4}$$

$$Ra = \frac{g\beta d^3(\overline{T_p} - T_1)}{\alpha v} \tag{5}$$

$$h_{c,p-1} = \frac{Nuk_{air}}{d} \tag{6}$$

where θ is the collector tilt relative to the horizontal, R_a is the Rayleigh number, g is the gravity, β is the thermal expansion coefficient, d is the distance between the absorber plate and glass, α is the thermal diffusivity, v is the kinematic viscosity, and k_{air} is the thermal conductivity of air.

The convective heat transferred from the absorber plate to the glass of dy is:

$$\delta q_{c,p-1} = W\left(\overline{T_p} - T_1\right)h_{c,p-1}dy \tag{7}$$

The radiative heat transferred from the glass to the sky of dy is as follows [16]:

$$\delta q_{r,1-a} = \sigma\varepsilon_1 W\left(T_1^4 - T_{sky}^4\right)dy \tag{8}$$

where the temperature of the sky is $T_{sky} = 0.0552T_a^{1.5}$.

The convective heat transfer coefficient between the glass and the environment is as follows [17]:

$$h_w = 5.7 + 3.8V_a \tag{9}$$

where V_a is the wind speed.

The convective heat transferred from the glass to the environment of dy is:

$$\delta q_{c,1-a} = Wh_w\left(T_1 - T_a\right)dy \tag{10}$$

The following equation must hold in steady state:

$$\delta q_{r,p-1} + \delta q_{c,p-1} = \delta q_{r,1-a} + \delta q_{c,1-a} \tag{11}$$

The top local heat loss coefficient of dy $\overline{U}_{l,t}$ is:

$$\overline{U}_{l,t} = \frac{\delta q_{r,p-1} + \delta q_{c,p-1}}{W(\overline{T_p} - T_a)dy} \tag{12}$$

The heat loss coefficient consists of the top, back, and edge heat loss coefficients.

The back heat loss coefficient is calculated as follows [18]:

$$U_b = \frac{k_l}{L_b} \tag{13}$$

where k_l is the thermal conductivity of the insulation material and L_b is the thickness of the insulation material in back.

The edge heat loss coefficient is estimated as follows [18]:

$$U_e = \frac{k_l A_e}{L_e A_p} \tag{14}$$

where A_e is the side area of the collector and L_e is the thickness of the insulation material at the side.

The local heat loss coefficient of *dy* is as follows [18]:

$$\overline{U}_l = \overline{U}_{l,t} + U_b + U_e \tag{15}$$

According to Equations (3) to (15), if $\overline{T_p}$ is known, $\overline{U_l}$ can be calculated by a numerical method.

Given that the fin thickness is smaller than the width, the temperature gradient in the direction of the fin thickness is neglected. The temperature distribution of the fin in the *x* direction is as follows [18]:

$$\frac{T_n - T_a - \dfrac{S}{\overline{U_l}}}{T_b - T_a - \dfrac{S}{\overline{U_l}}} = \frac{\cosh Bx}{\cosh \dfrac{B(W - D_o)}{2}} \tag{16}$$

where T_n is the fin temperature, $B = \sqrt{\overline{U_l}/(\lambda\delta)}$, λ is the thermal conductivity of the fins, δ is the fin thickness, T_b is the metal tube temperature, and D_o is the metal tube outer diameter.

In the steady state, the heat obtained by the absorber plate is equal to the heat obtained by the metal tube and fins. The heat obtained by *dy* is as follows [14,18]:

$$\delta q_u' = WF'\left[S - \overline{U_l}\left(T_f - T_a\right)\right]dy \tag{17}$$

$$F' = \frac{1}{\dfrac{W\overline{U_l}}{\pi D_i h_{f,i}} + \dfrac{W}{D_o + (W - D_o)\eta_n}} \tag{18}$$

where F' is the collector efficiency factor, T_f is the fluid temperature, D_i is the metal tube inner diameter, and $h_{f,i}$ is the convective heat transfer coefficient between the metal tube and fluid.

Fin efficiency can be determined as follows [18]:

$$\eta_n = \tanh\left[B(W - D_o)/2\right] / \left[B(W - D_o)/2\right] \tag{19}$$

The heat obtained by the absorber plate is finally transferred to the fluid, thermal contact resistance is neglected, and $\delta q_u'$ can be expressed as follows [18]:

$$\delta q_u' = \left(\frac{T_b - T_f}{\dfrac{1}{\pi D_i h_{f,i}}}\right)dy \tag{20}$$

The relationship between the metal tube and fluid temperatures can then be deduced by Equations (17)–(20):

$$T_b = \frac{WF'\left[S - \overline{U_l}\left(T_f - T_a\right)\right]}{\pi D_i h_{f,i}} + T_f \tag{21}$$

According to Equation (21), if T_f is defined by an assumed initial value and $\overline{U_l}$ is calculated by assumed $\overline{T_p}$, then T_b can be computed. Substituting T_b into Equation (16) yields the relationship between T_n and x:

$$T_n = \left[\frac{\cosh Bx}{\cosh\frac{B(W-D_o)}{2}}\right]\left(T_b - T_a - \frac{S}{\overline{U_l}}\right) + T_a + \frac{S}{\overline{U_l}} \tag{22}$$

The average fin temperature of *dy* I s:

$$\overline{T_n} = \frac{\int_0^{\frac{W-D_o}{2}} T_n dx}{\frac{W-D_o}{2}} \tag{23}$$

The average temperature of *dy* is:

$$\overline{T_p} = \frac{D_o T_b + (W-D_o)\overline{T_n}}{W} \tag{24}$$

Figure 2. Flow chart of simulation program for evaluating $\overline{U_l}$.

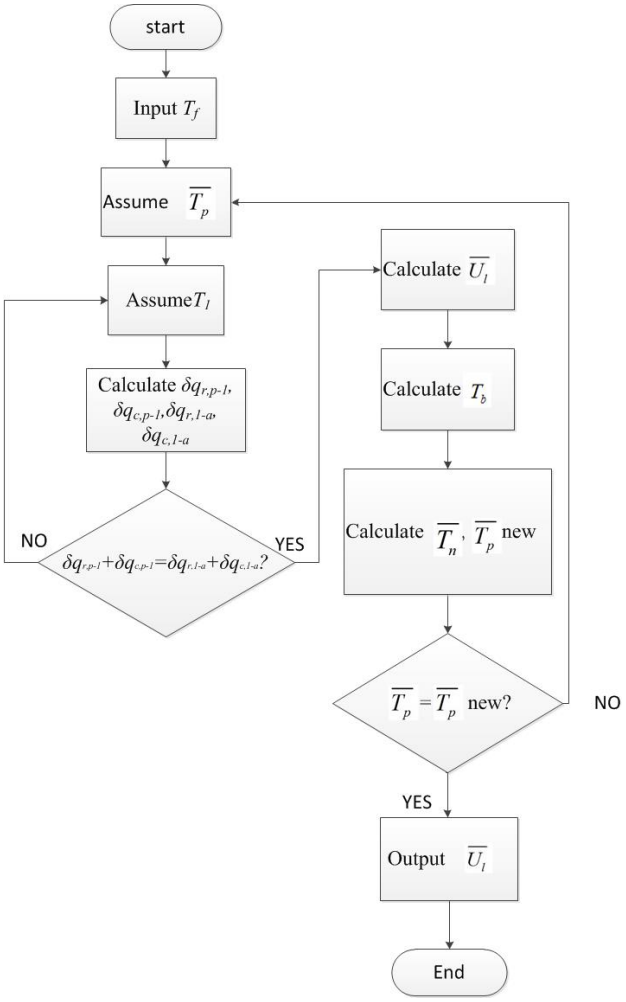

From Equation (24), the calculated value of $\overline{T_p}$ can be obtained. If the difference between the calculated value of $\overline{T_p}$ and the assumed value is greater than the admissible error, then another value of $\overline{T_p}$ is assumed until the difference is less than the admissible error and the correctly assumed $\overline{T_p}$ is considered the correct value. The correct value of $\overline{U_l}$ is the output. The calculation procedure of $\overline{U_l}$ is illustrated in Figure 2.

According to this method, if T_f is set to several values, then different corresponding values of $\overline{U_l}$ can be obtained. As a result, the function of T_f and $\overline{U_l}$ can be established by the least-square fitting method:

$$T_f = f\left(\overline{U_l}\right) \tag{25}$$

The energy equation of *dy* in the fluid flow direction can be expressed as:

$$q_u' = \frac{m}{n} c_p dT_f \tag{26}$$

where m is the fluid mass flow rate, n is the metal tube number of collectors, and c_p is the heat capacity of the fluid.

Substituting Equation (17) into Equation (26) yields the following:

$$\int_{T_i}^{T_f} \frac{mc_p}{nWF'\left[S - \overline{U_l}\left(T_f - T_a\right)\right]} dT_f = \int_0^y dy \tag{27}$$

where T_i is the fluid inlet temperature.

Equation (27) shows the relationship between T_f and y. Substituting Equation (25) into Equation (27) yields the relationship between $\overline{U_l}$ and y:

$$\overline{U_l} = g\left(y\right) \tag{28}$$

The average heat loss coefficient is:

$$\overline{\overline{U_l}} = \frac{\int_0^L \overline{U_l} dy}{L} = U_L \tag{29}$$

where L is the metal tube length and U_L is the overall heat loss coefficient.

Substituting $\overline{\overline{U_l}}$ into Equations (3) to (15) yields the average absorber plate temperature $\overline{\overline{T_p}}$.

2.3. Exergy Analysis

The equation of exergy balance takes the following form [8,19]:

$$E_{in} - E_s - E_{out} - E_d = 0 \tag{30}$$

where E_{in} is the inlet exergy rate, E_s is the stored exergy rate, E_{out} is the outlet exergy rate, and E_d is the exergy loss rate.

At steady conditions, $E_s = 0$.

The inlet exergy rate consists of the inlet exergy carried by fluid flow and the radiation exergy rate from the sun. The rate of inlet exergy carried by fluid flow is as follows [20,21]:

$$E_{in,f} = mc_p(T_i - T_a - T_a \ln(\frac{T_i}{T_a})) \tag{31}$$

The radiation exergy rate from the sun on the collector surface can be calculated as follows [6]:

$$E_{in,Q} = IA_c(1 - \frac{T_a}{T_s}) \tag{32}$$

where I is the solar irradiance and A_c is the aperture area. The apparent solar temperature as exergy source T_s is assumed to be 4350 K [11].

The rate of outlet exergy carried by fluid flow is as follows [20,21]:

$$E_{out,f} = mc_p(T_o - T_a - T_a \ln(\frac{T_o}{T_a})) \tag{33}$$

where T_o is the fluid outlet temperature.

The exergy loss rate consists of the following four parts:

The first part of the exergy loss rate is caused by heat leakage from the absorber plate to the environment [3]:

$$E_l = U_L A_p(\overline{\overline{T_p}} - T_a)(1 - \frac{T_a}{\overline{\overline{T_p}}}) \tag{34}$$

The second part of the exergy loss rate is caused by the temperature difference between the absorber plate surface and the Sun [3]:

$$E_{d1} = (\tau\alpha)_e IA_p T_a(\frac{1}{\overline{\overline{T_p}}} - \frac{1}{T_s}) \tag{35}$$

where $(\tau\alpha)_e$ is the effective product transmittance–absorptance.

The third part of the exergy loss rate is due to solar radiation losses from the collector surface to the absorber plate:

$$E_{d2} = I\left[A_c - (\tau\alpha)_e A_p\right](1 - \frac{T_a}{T_s}) \tag{36}$$

The fourth part of the exergy loss rate is caused by the temperature difference between the absorber plate and fluid [21]:

$$E_{d3} = mc_p T_a\left[\ln(\frac{T_o}{T_i}) - \frac{(T_o - T_i)}{\overline{\overline{T_p}}}\right] \tag{37}$$

According to Equations (30) to (37), the useful exergy rate is:

$$E_u = E_{out,f} - E_{in,f} \tag{38}$$

Solar collector exergy efficiency is calculated by dividing the increase in fluid flow exergy by the inlet radiation exergy [9]:

$$\eta_{ex} = \frac{E_{out,f} - E_{in,f}}{IA_c(1 - \frac{T_a}{T_s})} \tag{39}$$

According to Equations (30)–(37), the fluid outlet temperature T_o can be obtained. Substituting relevant data into Equations (34)–(39) yields the useful exergy rate, exergy loss rate, and exergy efficiency.

3. Validation of Methodology

Experiments are conducted to validate the methodology. The flat plate collector is Sangpu PYT/L2.0-3, the metal tubes are made of copper, the fins are made of aluminum, the insulation material is rock wool board, and the working fluid is water. The relative parameters of the flat plate collector are listed in Table 1.

Table 1. Parameters of the flat plate collector.

Parameter	Value
Tube center to center distance	0.135 m
The metal tube length	2 m
The metal tube number of collectors	7
The metal tube outer diameter	0.015 m
Thermal conductivity of the fins	236 W/(m·K)
Thermal conductivity of the insulation material	0.055 W/(m·K)
Effective product transmittance–absorptance	0.88
Emissivity of the absorber plate	0.05
Emissivity of the glass	0.88
Size of the flat plate collector	2 m × 1 m ×0.07 m
Collector tilt relative to the horizontal	45°

The experimental test platform is shown in Figure 3.

Figure 3. Experimental test platform.

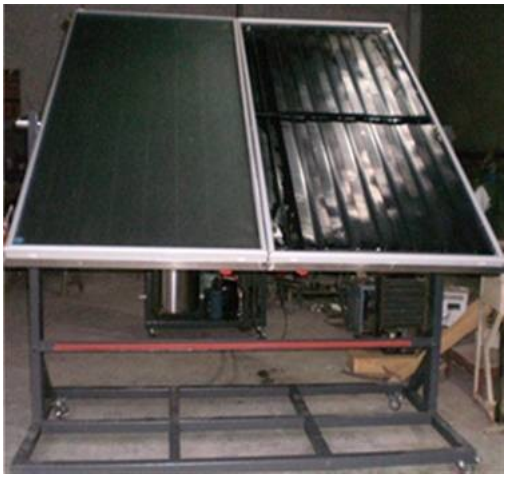

The values calculated by the above method and experimental data are compared, and the results are shown in Table 2.

Table 2. Comparison between calculated values and experimental data.

	Time					
	10–11	11–12	12–13	13–14	14–15	15–16
I/(W/m^2)	631	702	713	640	535	374
T_a/°C	25.5	26.4	27.7	27.5	26.8	25.7
T_i/°C	29.4	37.3	44.6	51.9	61.1	67.2
$\eta_{ex.calc}$/%	1.56	3.09	4.10	4.85	4.86	2.44
$\eta_{ex.exp}$/%	1.62	2.96	3.95	4.79	4.90	2.59
E_{exergy}/%	3.70	4.39	3.80	1.25	0.82	5.79

An experiment is conducted in six time segments of a day. The fluid inlet temperature is controlled by an electrically heated constant-temperature water bath. The fluid inlet temperature of each measurement is different, and the mass flow rate is controlled at 0.05 kg/s by adjusting the valve. When the collector is in steady state (*i.e.*, ambient temperature: ± 1 °C; solar irradiance: ± 50 W/m^2; fluid inlet temperature: ± 0.1 °C; fluid mass flow rate: ± 1%), the experimental data are collected. Four independent data acquisition procedures are conducted for each individual test point, and the collection intervals are at least 3 minutes long. $\eta_{ex.calc}$ is the calculated exergy efficiency, $\eta_{ex.exp}$ is the experimental efficiency, and E_{exergy} is the relative error. Table 2 shows that only a small difference was observed between the calculated values and experimental results.

4. Results and Discussion

With the suggested calculation method of this study, the effects of ambient temperature, solar irradiance, fluid mass flow rate, and fluid inlet temperature on the useful heat rate, useful exergy rate, and exergy loss rate are examined.

Figure 4 shows the following conditions: (1) The useful heat rate increases with increasing ambient temperature because of decreasing heat loss. (2) The useful exergy rate decreases with increasing ambient temperature, indicating that increasing ambient temperature decreases exergy efficiency. (3) The exergy loss rate caused by heat leakage from the absorber plate to the environment decreases with increasing ambient temperature. This condition can be attributed to the increase in ambient temperature leading to a decrease in heat losses from the solar collector to the environment and consequently to a decrease in E_l. (4) The exergy loss rate caused by the temperature difference between the absorber plate surface and the sun increases with increasing ambient temperature. Although an increase in ambient temperature increases $\overline{\overline{T_p}}$, the increasing tendency of $\overline{\overline{T_p}}$ is less than that of the ambient temperature. Consequently, increasing ambient temperature increases E_{d1}. (5) The exergy loss rate because of solar radiation losses from the collector surface to the absorber plate decreases slowly with increasing ambient temperature because the increment of ambient temperature is small relative to T_s. (6) The exergy loss rate caused by the temperature difference between the absorber plate and fluid increases with increasing ambient temperature because an increase in ambient temperature increases $\overline{\overline{T_p}}$ and consequently increases the temperature difference between the absorber plate and fluid.

Figure 4. Variations of useful heat rate, useful exergy rate, and exergy loss rate *versus* ambient temperature.

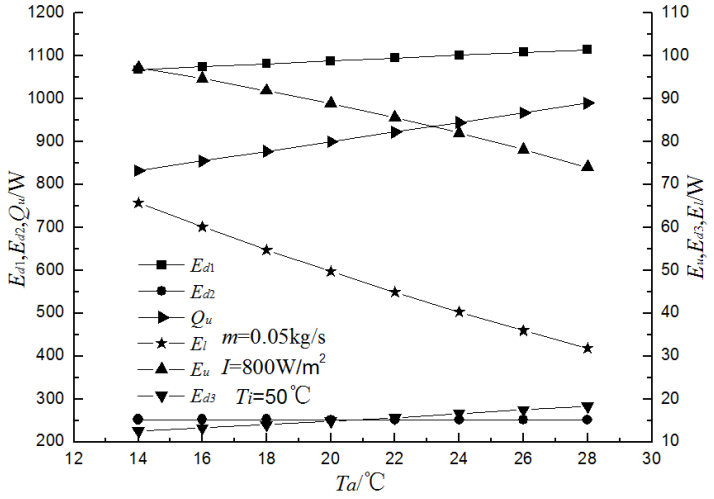

The useful heat rate and useful exergy rate have conflicting behavior with increasing ambient temperature. Although E_l decreases from 65.7 W to 31.8 W with ambient temperature increasing from 14 °C to 28 °C (the reduction proportion is more than 50%), E_u decreases from 97.2 W to 74.0 W because of increasing E_{d1} and E_{d3} and decreasing $E_{in,Q}$.

Figure 5 shows that the increase in solar irradiance increases the useful heat rate, useful exergy rate, and exergy loss rate. Q_u has the largest increment, increasing from 149.6 W to 1199.0 W with solar irradiance increasing from 300 W to 1000 W. E_{d1} has an increment of 417.1 W to 1347.3 W, but E_u increases from 14.0 W to 120.8 W. Solar irradiance significantly affects both the useful heat rate and useful exergy rate. Appropriate solar irradiance can improve collector performance effectively.

Figure 5. Variations of useful heat rate, useful exergy rate and exergy loss rate *versus* solar irradiance.

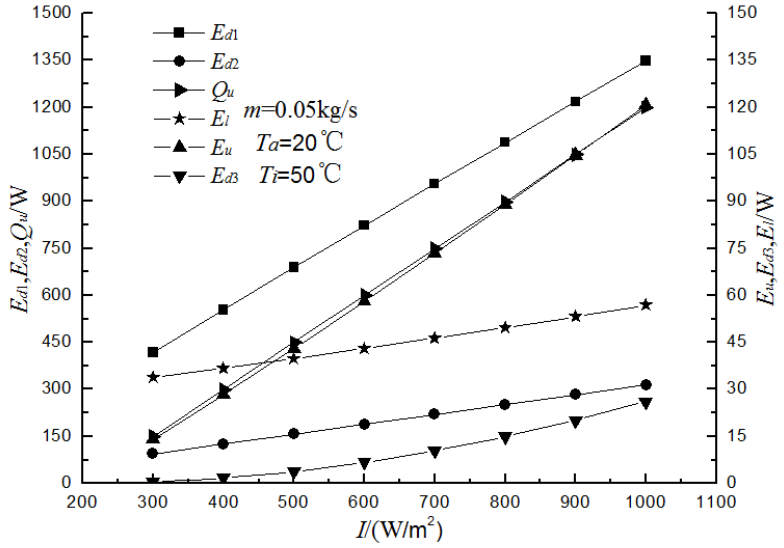

The variations of the useful heat rate, useful exergy rate, and exergy loss rate *versus* fluid inlet temperature are illustrated in Figure 6, leading to the following conclusions: (1) the useful heat rate

decreases with increasing fluid inlet temperature because of increasing heat loss; (2) an optimum fluid inlet temperature exists for obtaining the maximum useful exergy rate. The useful exergy rate first increases and then decreases with increasing fluid inlet temperature. It reaches its maximum when the fluid inlet temperature is 69 °C because the increase in fluid inlet temperature increases both the average absorber plate temperature and fluid outlet temperature. When the fluid inlet temperature is low, increasing fluid outlet temperature considerably affects E_u, which increases with increasing fluid inlet temperature. However, while the fluid inlet temperature is higher than the optimized value, the increasing heat loss caused by the increasing average absorber plate temperature significantly affects E_u, which then decreases; (3) the exergy loss rate caused by heat leakage from the absorber plate to the environment increases with increasing fluid inlet temperature because the increase in fluid inlet temperature increases the average absorber plate temperature and consequently increases heat losses from the solar collector to the environment, thereby increasing E_l; (4) the exergy loss rate caused by the temperature difference between the absorber plate surface and the sun decreases with increasing fluid inlet temperature because the increase in fluid inlet temperature increases the average absorber plate temperature and consequently decreases the temperature difference of radiative heat transfer, thereby reducing E_{d1}; (5) the fluid inlet temperature has no effect on the exergy loss rate because of the solar radiation losses from the collector surface to the absorber plate. This part of the exergy loss rate remains constant with increasing fluid inlet temperature; (6) the exergy loss rate caused by the temperature difference between the absorber plate and fluid decreases with increasing fluid inlet temperature because the increase in fluid inlet temperature decreases the temperature difference of the absorber plate and fluid and consequently decreases this part of the exergy loss rate.

Figure 6. Variations of useful heat rate, useful exergy rate, and exergy loss rate *versus* fluid inlet temperature.

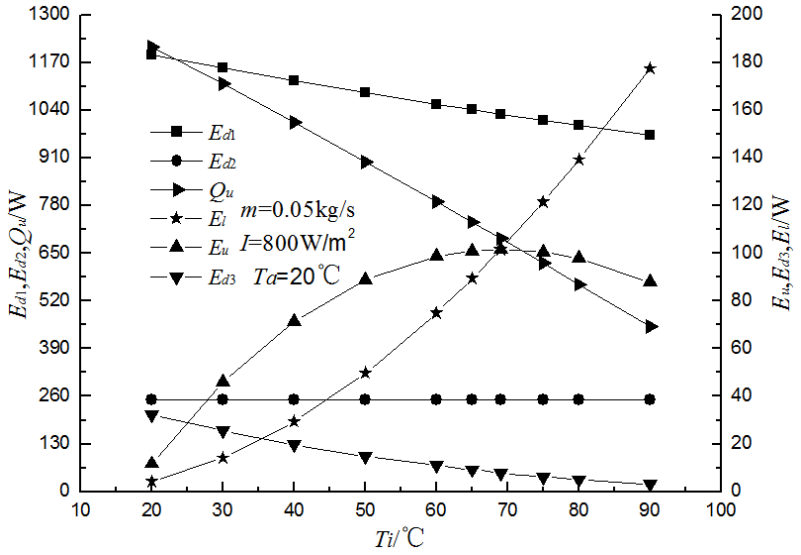

The useful heat rate and useful exergy rate also have conflicting behavior with increasing fluid inlet temperature. Q_u is high when fluid inlet temperature is low, but E_u is only 11.8 W when the fluid inlet temperature is 20 °C. E_u increases significantly with increasing fluid inlet temperature, even to its maximum. The maximum E_u is 101.6 W, and a significant exergy performance improvement is

observed. The optimum fluid inlet temperature varies. It is mainly affected by heat loss because of the flat plate collector's structure. E_l increases rapidly from 4.3 W to 177.5 W when fluid inlet temperature rises from 20 °C to 90 °C. Selecting appropriate evaluation criteria for the collector based on specific conditions and allowing the collector to work with appropriate fluid inlet temperature are recommended.

Figure 7 shows the variations of the useful heat rate, useful exergy rate, and exergy loss rate *versus* the fluid mass flow rate. The following conclusions are drawn: (1) the useful heat rate increases with increasing fluid mass flow rate because of decreasing heat loss, and the increasing tendency decreases; (2) from Figure 7(a), when the fluid inlet temperature is lower than the optimized value, the useful exergy rate decreases with increasing fluid mass flow rate and the decreasing tendency decreases because the increase in the fluid mass flow rate decreases the fluid outlet temperature. When the fluid inlet temperature is low, the decreasing fluid outlet temperature greatly affects E_u, which then decreases.

Figure 7. Variations of useful heat rate, useful exergy rate, and exergy loss rate *versus* fluid mass flow rate.

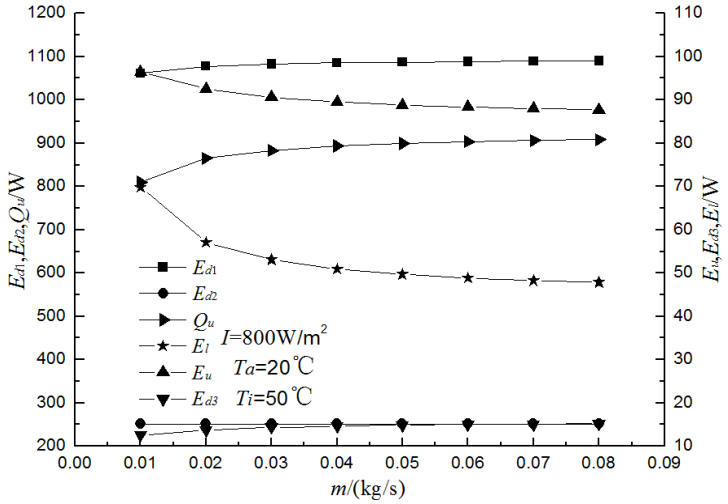

(a)

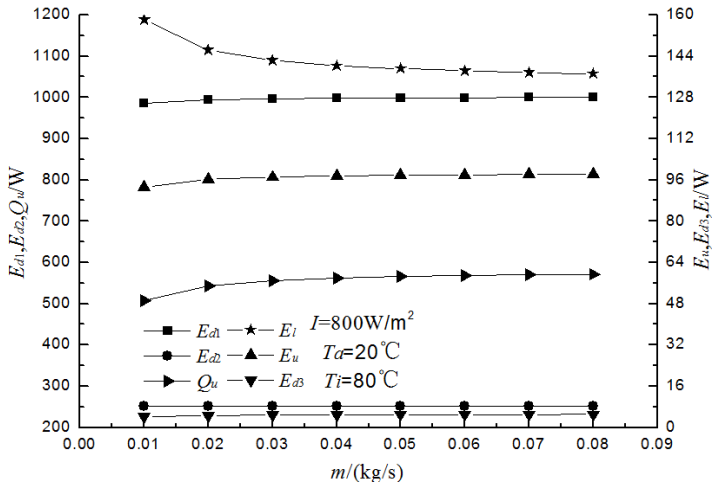

(b)

From Figure 7b, when the fluid inlet temperature is higher than the optimized value, the useful exergy rate increases with increasing fluid mass flow rate and the increasing tendency declines because increasing heat loss significantly affects E_u at this condition and increasing fluid mass flow rate

decreases heat losses from the solar collector to the environment; (3) the exergy loss rate caused by heat leakage from the absorber plate to the environment decreases with increasing fluid mass flow rate and the decreasing tendency decreases because the increase in fluid mass flow rate decreases the average absorber plate temperature and consequently decreases heat losses from the solar collector to the environment; (4) The exergy loss rate caused by the temperature difference between the absorber plate surface and the sun increases with increasing fluid mass flow rate and the increasing tendency decreases because the increase in fluid mass flow rate decreases the average absorber plate temperature and consequently increases the temperature difference of radiative heat transfer. Thus, this part of the exergy loss rate increases; (5) the fluid mass flow rate has no effect on the exergy loss rate because of solar radiation losses from the collector surface to the absorber plate. This part of the exergy loss rate remains constant with increasing fluid mass flow rate; (6) the exergy loss rate caused by the temperature difference between the absorber plate and the fluid increases with increasing fluid mass flow rate because the increase in the fluid mass flow rate increases the heat transfer between the absorber plate and fluid and consequently increases this part of the exergy loss rate.

When the fluid inlet temperature is lower than the optimized value, the variation trends of Q_u and E_u are opposite those of the increasing fluid mass flow rate. When the fluid inlet temperature is higher than the optimized value, the variation trends of Q_u and E_u are the same. Notably, the effect of the mass flow rate on performance declines with increasing mass flow rate. The mass flow rate should be carefully controlled based on actual demand. Table 3 shows the exergy rate distribution of the collector when T_a = 20 °C, I = 800 W/m^2, m = 0.05 kg/s, T_i = 50 °C. Percentage = $E_x/(E_u+E_{d1}+E_{d2}+E_{d3}+E_l)$. Table 3 shows the following conditions: (1) the percentage of useful exergy rate (*i.e.*, exergy efficiency) is 5.96%; (2) the largest exergy loss of the collector is the exergy loss rate caused by the temperature difference between the absorber plate surface and the sun, accounting for 72.87% of the total exergy rate; (3) the percentage of the exergy loss rate because of solar radiation losses from the collector surface to the absorber plate is 16.84%, mainly affected by the glass material and selective-absorption coating; (4) the percentage of the exergy loss rate caused by the temperature difference between the absorber plate and fluid and that caused by heat leakage from the absorber plate to the environment are 1% and 3.33%, respectively.

Table 3. Exergy rate distribution of collector.

Exergy Rate	Value/W	Percentage/%
E_u	88.860	5.96
E_{d1}	1087.427	72.87
E_{d2}	251.282	16.84
E_{d3}	14.880	1.00
E_l	49.713	3.33

5. Conclusions

In this study, the first and second laws of thermodynamics are used to study the performance of a flat plate solar collector. A theoretical model for the exergy analysis of flat plate collectors is presented by considering non-uniformity in the temperature distribution of the absorber plate:

(1) The model is experimentally validated, with the results agreeing well with the experimental data.
(2) The useful heat rate increases with increasing ambient temperature, solar irradiance, and fluid mass flow rate and decreases with increasing fluid inlet temperature.
(3) The effects of ambient temperature, solar irradiance, fluid inlet temperature, and fluid mass flow rate on useful exergy rate and exergy loss rate are obtained. The conclusion can be summarized as follows: the useful exergy rate decreases with increasing ambient temperature and increases with increasing solar irradiance. It first increases and then decreases with increasing fluid inlet temperature, and an optimum fluid inlet temperature exists for obtaining the maximum useful exergy rate. When the fluid inlet temperature is lower than the optimized value, the useful exergy rate then decreases with increasing fluid mass flow rate. However, when the fluid inlet temperature is higher than the optimized value, the useful exergy rate increases with increasing fluid mass flow rate, the effect of mass flow rate on performance decreases with increasing mass flow rate, and the mass flow rate should be controlled carefully based on actual demand.
(4) The useful heat rate is greater than the useful exergy rate. The useful heat rate and useful exergy rate have conflicting behavior in many cases. Thus, selecting an appropriate evaluation criterion (energy or exergy) for the collector according to specific conditions is recommended.
(5) Solar irradiance considerably affects both the useful heat rate and useful exergy rate. In other words, high performance is based on appropriate solar irradiance.
(6) The optimum fluid inlet temperature varies, and it is mainly affected by heat loss because environmental parameters change during the day. The operating parameters could be adjusted to obtain the maximum useful exergy rate during the day, and exergy performance could be significantly improved by optimizing it.
(7) The exergy loss rate caused by the temperature difference between the absorber plate surface and the sun accounts for the largest exergy loss of the collector. When T_a = 20 °C, I = 800 W/m^2, m = 0.05 kg/s, and T_i = 50 °C, it accounts for 72.87% of the total exergy rate.

Based on this analysis, the appropriate operating conditions for collectors could be determined with the given conditions and are useful for obtaining a higher useful exergy rate and decreasing internal irreversibilities.

Acknowledgments

The study presented in this paper is financially supported by National Natural Science Foundation Programs of China (Grant Nos. 51066002, 51366005, U0937604), Yunnan Provincial Natural Science Foundation Programs (Grant Nos. 2008KA002, 2008CD001), high-tech development project by the Development and Reform Commission of Yunnan province (Grant Nos .2008CD001) and Applied Basic Research Projects of Yunnan Province(Grant Nos. KKSY201252024).

Author Contributions

Huitao Wang and Zhong Ge contributed to the conception of the study. Huitao Wang and Zhong Ge contributed to the building of model. Hua Wang, Songyuan Zhang and Xin Guan designed the experiment. Zhong Ge, Songyuan Zhang contributed to the data collecting. Zhong Ge performed the

data analyses and wrote the manuscript. Hua Wang and Huitao Wang helped in the analysis with constructive discussions.

Nomenclature

Roman symbols

A_c	the aperture area	m^2
A_e	the side area of the collector	m^2
A_p	the area of the absorber plate	m^2
c_p	the heat capacity of the fluid	J/(kg·K)
d	the distance between the absorber plate and glass	m
D_i	the metal tube inner diameter	m
D_o	the metal tube outer diameter	m
E_d	the exergy loss rate	W
E_{d1}	exergy loss rate caused by temperature difference between the absorber plate surface and the Sun	W
E_{d2}	exergy loss rate because of solar radiation losses from the collector surface to the absorber plate	W
E_{d3}	exergy loss rate caused by the temperature difference between the absorber plate and fluid	W
E_{in}	the inlet exergy rate	W
$E_{in,f}$	the inlet exergy rate carried by fluid flow	W
$E_{in,Q}$	the radiation exergy rate from the sun on the collector surface	W
E_l	exergy loss rate caused by heat leakage from the absorber plate to the environment	W
E_{out}	the outlet exergy rate	W
$E_{out,f}$	the outlet exergy rate carried by fluid flow	W
E_s	the stored exergy rate	W
E_u	the useful exergy rate	W
F'	the collector efficiency factor	
g	the gravity	m^2/s
$h_{c,p-1}$	the convective heat transfer coefficient between the absorber plate and the glass	$W/(m^2·K)$
$h_{f,i}$	the convective heat transfer coefficient between the metal tube and fluid	$W/(m^2·K)$
h_w	the convective heat transfer coefficient between the glass and the environment	$W/(m^2·K)$
I	the solar irradiance	W/m^2
k_{air}	the thermal conductivity of air	W/(m·K)
k_l	the thermal conductivity of the insulation material	W/(m·K)
L	the metal tube length	m
L_b	the thickness of the insulation material in back	m
L_e	the thickness of the insulation material at the side	m
m	the fluid mass flow rate	kg/s

n	the metal tube number of collectors	
Nu	the Nusselt number	
$\delta q_{c,p-1}$	the convective heat transfer from the absorber plate to the glass of dy	W
$\delta q_{c,1-a}$	the convective heat transfer from the glass to the environment of dy	W/(m^2·K)
$\delta q_{r,p-1}$	the radiative heat transfer from the absorber plate to the glass of dy	W
$\delta q_{r,1-a}$	the radiative heat transfer from the glass to the sky of dy	W
$\delta q_u'$	the heat obtained by dy	W
Q_l	the heat loss from the solar collector to the environment	W
Q_s	the radiation flux absorbed by the absorber plate	W
Q_u	the useful heat rate gain of the flat plate solar collector	W
R_a	the Rayleigh number	
S	the radiation flux absorbed by a unit area of the absorber plate	W/m^2
T_a	the ambient temperature	K
T_b	the metal tube temperature	K
T_f	the fluid temperature	K
T_i	the fluid inlet temperature	K
T_n	the fin temperature	K
T_o	the fluid outlet temperature	K
T_p	the temperature of dA	K
$\overline{T_p}$	the average temperature of dy	K
$\overline{\overline{T_p}}$	the integral average of T_p over the absorber plate	K
T_s	the apparent solar temperature as exergy source	K
T_{sky}	the temperature of the sky	K
T_l	the temperature of the glass	K
U_b	the back heat loss coefficient	W/(m^2·K)
U_e	the edge heat loss coefficient	W/(m^2·K)
U_l	the local heat loss coefficient of dA	W/(m^2·K)
$\overline{U_l}$	the local heat loss coefficient of dy	W/(m^2·K)
$\overline{U}_{l,t}$	the top local heat loss coefficient of dy	W/(m^2·K)
$\overline{\overline{U_l}}$	the integral average of U_l over the absorber plate	W/(m^2·K)
U_L	the overall heat loss coefficient	W/(m^2·K)
v	the kinematic viscosity	m^2/s
V_a	the wind speed	m/s
W	the width of the metal tube and fins	m
Greek		
α	the thermal diffusivity	m^2/s
β	the thermal expansion coefficient	1/K
δ	the fin thickness	m
ε_p	the emissivity of the absorber plate	
ε_l	the emissivity of the glass	
η_{ex}	the exergy efficiency	

η_n	the fin efficiency	
θ	the collector tilt relative to the horizontal	°
λ	the thermal conductivity of the fins	W/(m·K)
σ	the Stefan–Boltzmann constant	$W/(m^2 \cdot K^4)$
$(\tau\alpha)_e$	the effective product transmittance–absorptance	

Conflicts of Interest

The authors declare no conflict of interest.

References

1. Zhai, R.R.; Zhu, Y.; Yang Y.P.; Tan, K.Y.; Eric, H. Exergetic and Parametric Study of a Solar Aided Coal-Fired Power Plant. *Entropy* **2013**, *15*, 1014–1034.
2. Fahad, A.A.; Ibrahim, D.; Feridum, H. Exergy modeling of a new solar driven trigeneration system. *Sol. Energ*. **2011**, *85*, 2228–2243.
3. Dutta, G.K.K.; Saha, S.K. Energy analysis of solar thermal collectors. *Renew. Energ. Environ*. **1990**, *33*, 283–287.
4. Tyagi, S.K.; Wang, S.W.; Singhal, M.K.; Kaushik, S.C.; Park, S.R. Exergy analysis and parametric study of concentrating type solar collectors. *Int. J. Therm. Sci*. **2007**, *46*, 1304–1310.
5. Liu, G.; Cengel Y.A.; Turner R.H. Exergy analysis of a solar heating system. *J. Sol. Energ*. **1995**, *117*, 249–251.
6. Torres-Reyes, E.; Cervantes de Gortari, J.G.; Ibarra-Salazar, B.A.; Picon-Nunez, M.A. design method of flat-plate solar collectors based on minimum entropy generation. *Exergy* **2001**, *1*, 46–52.
7. Bejan, A.; Keary, D.W.; Kreith, F. Second law analysis and synthesis of solar collector systems. *J. Sol. Energ*. **1981**, *103*, 23–28.
8. Suzuki, A. A fundamental equation for exergy balance on solar collectors. *J. Sol. Energ*. **1988**, *110*, 102–106.
9. Farzad, J.; Emad, A. Energetic and exergetic evaluation of flat plate solar collectors. *Renew. Energ*. **2013**, *56*, 55–63.
10. Luminosua, I.; Fara, L. Determination of the optimal operation mode of a flat solar collector by exergetic analysis and numerical simulation. *Energy* **2005**, *30*, 731–747.
11. Farahat, S.; Sarhaddi, F.; Ajam, H. Exergetic optimization of flat plate solar collectors. *Renew. Energ*. **2009**, *34*, 1169–1174.
12. Akpinar, E.K.; Koçyigit, F. Energy and exergy analysis of a new flat-plate solar air heater having different obstacles on absorber plates. *Appl. Energ*. **2010**, *87*, 3438–3450.
13. Altaa, D.; Bilgilib, E.; Ertekina, C.; Yaldiz, O. Experimental investigation of three different solar air heaters: Energy and exergy analyses. *Appl. Energ*. **2010**, *87*, 2953–2973.
14. Duffie, J.A.; Beckman, W.A. *Solar Engineering of Thermal Processes*; Wiley-Interscience: New York, NY, USA, 1991.
15. Dorfling, C.; Hornung, C.H.; Hallmark, B.; Beaumont, R.J.J.; Fovargue, H.; Mackley, M.R. The experimental response and modelling of a solar heat collector fabricated from plastic microcapillary films. *Sol. Energ. Mat. Sol. C* **2010**, *94*, 1207–1221.

16. Incropera, F.P.; DeWitt, D.P. *Fundamentals of Heat and Mass Transfer*; JohnWiley and Sons: New York, NY, USA, 1990.
17. Taherian, H.; Rezania, A.; Sadeghi, S.; Ganjia, D.D. Experimental validation of dynamic simulation of the flat plate collector in a closed thermosyphon solar water heater. *Energ. Convers. Manag*. **2011**, *52*, 301–307.
18. Zhang, H.F. *Solar Thermal Utilization Principles and Computer Simulation*; Northwestern Polytechnical University Press: Xi'an, China, 2004.
19. Suzuki, A. General theory of exergy balance analysis and application to solar collectors. *Energy* **1988**, *13*, 153–160.
20. Kotas, T.J. *The Exergy Method of Thermal Plant Analysis*; Krieger Publish Company: Malabar, FL, USA, 1995.
21. Bejan, A. *Advanced Engineering Thermodynamics*; Wiley Interscience: New York, NY, USA, 1988.